Available online at www.sciencedirect.com
ScienceDirect
Physics Procedia 5 (2010) 607–615
Physics Procedia
www.elsevier.com/locate/procedia

LANE 2010

Functionality of Laser-Sintered Shape Memory Micro-Actuators

S. Dudziak*, M. Gieseke, H. Haferkamp, S. Barcikowski, D. Kracht

Laser Zentrum Hannover e. V., Hollerithallee 8, 30419 Hannover, Germany

Abstract

NiTi shape memory alloys are considered to be difficult to machine. Dimensional accuracy can hardly be met especially in micro-machining. Being a non-contact tool and therefore independent from machining forces, the laser is a promising alternative for manufacturing NiTi micro-parts. This paper presents research results on powder bed-based laser sintering of fine NiTi powders. Structures with a minimum width of approximately 50 µm can be generated without losing the special shape memory properties. The structures "remember" the shape which was set in the laser process. We show that phase transformation temperature can be influenced by process parameters.

Keywords: rapid manufacturing; laser sintering; shape memory alloys; nickel; titanium; one-way effect

1. Introduction

The generation of micro-actuators made of nickel-titanium (NiTi) shape memory alloys is considered to be a challenge [1, 2], since the machinability of NiTi materials is difficult [3, 4]. NiTi materials show high ductility leading to disadvantageous chip formation and breakage, burr formation and strong adhesion between the tool and the work piece. Moreover, the material's distinct work hardening results in high tool wear. After grinding operations, the surface layer of small diameter workpieces, such as tubes and wires, has to be removed using an additional etching step, since shape memory properties are influenced in this work-hardened area. Especially in micro-machining, the high spring-back potential of NiTi shape memory alloys limits dimensional accuracy. As a non-contact tool, and therefore independent of machining forces and material-based tool wear, laser radiation is a promising alternative for the generation of micro-actuators made of NiTi [2, 5, 6]. In his review article [7], Bonsignore states that laser micromachining dominates the current practice of stent manufacturing, for example. For stent fabrication using laser cutting, NiTi tubes are generally available in a variety of small inner and outer diameters [8]. In contrast, the availability of raw material, except from tubes, wires or sheet, is limited [8, 9, 10].

* Corresponding author. Tel.: +49-511-2788-340.
E-mail address: s.dudziak@lzh.de.

1875-3892
doi:10.1016/j.phpro.2010.08.088

Moreover, NiTi material has a high price level. As a reason, Mertmann accounts the limited demand for NiTi products besides the well-established applications in medical engineering. Taking the technical user's view into account, Seitz [11] lists the sensitive and complex and therefore cost-intensive manufacturing technologies, limited knowledge of the material's behavior in application [12] and high material prices for limited demands, although the potential of the special functional properties of NiTi is well known. Thus, the vicious circle regarding raw material availability and price is closed.

One approach to clear the hurdles in the way to technical application, near-net-shape processing of NiTi using laser based processes, is under investigation [13, 14]. While limitations regarding spring-back of the workpiece and tool wear can be overcome, the challenges in laser processing deal with the sensitivity of NiTi to a change in the chemical composition of the material. It is well known that an increase in the nickel concentration by only 0.1 at% can cause a shift in the phase transformation temperature (PTT), at which the material remembers its original shape, by more than 10 K [15]. As NiTi alloys are highly reactive and easily pick up impurities during high temperature processing [16], changes in PTT resulting from a laser based process have to be controlled carefully. Regarding near-net-shape fabrication of NiTi parts from a powder bed, this is of particular importance, as powders show an increased surface in comparison to a dense part of the same volume. In order to generate micro-actuators from a powder bed and therefore to achieve a high structure resolution, only powder particles with a small medium diameter are used. As a result, impurity pick up on the powder particle surface, respectively impurity import into a dense micro-part has an even greater impact. This is due to the fact that the powder surface increases by the factor r_1/r_2, if r_2 is the medium diameter of the finer powder particles and r_1 the medium diameter of coarser powder particles. Therein, material's volume consistency of the powder portions compared and spherical powder particle geometry is assumed.

In the present work, we show results of investigations on laser sintering of NiTi powders with particle diameters $d < 25$ µm. In order to develop a manufacturing method for shape memory micro-actuators, focus is on the achievable structure resolution. The preservation of the shape memory functionality is of crucial importance.

2. Experimental Work

In order to generate homogeneous NiTi micro-parts, it was assumed to be most feasible to use prealloyed NiTi powders. As the availability of NiTi powder material is highly limited, the powder was produced by gas atomization from NiTi bar material, respectively cylindrical as-cast NiTi ingots. The bar material was purchased by Memry GmbH, Weil am Rhein, Germany. The bar material is a NiTi alloy with nominal austenite peak temperature (peak of the phase transformation in heating) of $A_{peak} = 84$ °C and a nickel content of around 49.8 to 50.0 at%. The surface of the bar material was in so-called "oxide free condition". The ingots were prepared by graphite crucible vacuum induction melting by Dr. Jan Frenzel, Institut für Werkstoffe, Ruhr-Universität Bochum (RUB). The initial nickel content in casting was 49.75 at%. Details of the RUB NiTi casting process are given in [17]. Five ingots were cast with A_{peak} temperatures varying between 97.9 °C and 112.9 °C. Both materials have been gas atomized under equal conditions by TLS Technik GmbH, Bitterfeld, Germany.

Laser sintered samples have been generated from the powder using a non-commercial laser micro-sintering system built at the Laser Zentrum Hannover e. V. (LZH). This system is equipped with a continuous wave Ytterbium fibre laser with a maximum output power $P_O = 25$ W, emitting laser radiation with a wavelength of $\lambda = 1072$ nm. The powder application system is adapted to deposit non-floatable powders of small diameters in the working plane. The process was carried out in an argon atmosphere. A NiTi base plate was used as a substrate material.

The morphology of the NiTi powders was investigated using scanning electron microscopy (CamScan Pioneer) and metallographic analysis. The distribution of the powder particle sizes for the powders used could not be analyzed using laser diffraction. This is due to the fact that the amount of powder particles gained from atomization in the desired range below 25 µm in diameter is limited to about 10 % to 15 %, resulting in only about 0.7 kg to 0.85 kg of fine NiTi powders. Complete powder handling in an argon atmosphere could not be guaranteed for the laser diffraction measurements. In order not to contaminate parts of the testing material, the size distribution measurement has so far not been carried out. The NiTi composition on pressed powder pallets was determined according to [13] using EDX with counting times of 600 s. The phase transformation behavior of the untreated powders as well as the

laser sintered samples was characterized using differential scanning calorimetry with a Perkin Elmer Pyris 1 DSC with a liquid nitrogen cooling unit. The samples were cycled on a temperature range between -120 °C and 130 °C, applying a heating respectively cooling rate of 10 K/min. As the weight of a single laser-sintered NiTi micro-test-specimen is far below the requested minimum sample weight for Pyris 1 of 5 mg, eight to twelve identically processed test specimens, generated from the same powder bed in one laser process, have been placed in one DSC sample pan.

3. Results and Discussion

3.1. NiTi powder material

Both powder materials have been delivered ordered by size. In this sorting process, particles smaller than d = 25 µm in diameter are separated from larger particles by sieving, and subsequently packed in a powder bottle under argon. The powder portions were analyzed regarding their morphology in as-received condition, first. A huge amount of the fine particles smaller than d = 25 µm in diameter could be found in the coarser powder fractions. For this reason, these portions of the powders made from the Memry bar material (in the following: NiTi-M) and from the ingots cast at RUB (NiTi-B) were subject to additional sieving processes using Retsch analysis sieves in an argon flooded sieving station. Doing so, the powders can be separated into particle portions > 100 µm, < 100 µm > 75 µm, < 75 µm > 45 µm, < 45 µm > 25 µm and < 25 µm in diameter. It was found that fine powder particles which should pass the 75-µm-sieve respectively the 45-µm-sieve adhere to each other and to the sieve mesh and therefore block it. For this reason, the sieves were cleaned after 60 minutes of operation, the powder portions were weight and filled back into the sieving station and the sieving process was repeated until the portions' amount did no longer change. Afterwards, the powder portions were investigated again. SEM photos of powder portions with nominal particle sizes < 45 µm > 25 µm and < 25 µm in diameter from NiTi-M and NiTi-B are shown in figure 1.

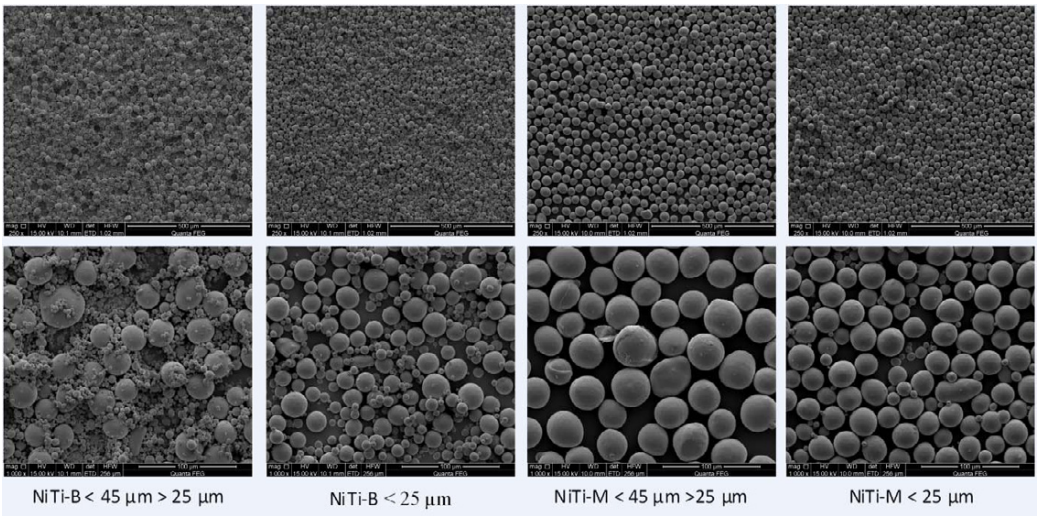

Fig. 1. SEM pictures of the named nominal powder particle fractions in 250 x respectively 1000 x magnification

This analysis provided the following results:

- The powder particles found in the sorted portions still do not match the sieved, nominal range in NiTi-B. Particles smaller than 25 µm in diameter can still be found in the portion which should contain only particles < 45µm > 25 µm in diameter.

- In this powder portion, the amount of fine particles with diameters below ca. 10 µm is even higher than in the portion which has passed the sieve with 25 µm mesh width. These fine particles form clusters which are placed in the spacing between coarser particles, which mostly resemble the addressed size (d = 25 µm – 45 µm). Finest particles found in this portion are as small as ca. 400 nm.
- The NiTi-B powder with a nominal diameter d < 25 µm is a homogeneous, multimodal powder, containing particles in a range of from 25 µm to about 1 µm in diameter.
- The powder particles found in the NiTi-M portion of a nominal range of d = 25 µm – 45 µm match the addressed size. No significantly smaller particles can be found.
- The main portion of NiTi-M powder particles with a nominal diameter d < 25 µm are in a size range > 15 µm < 25 µm in diameter. Compared to the NiTi-B portion, only a small amount of finer particles can be found, whereby the smallest particles are about 1 µm in diameter.

In summation, it can be said that the powders show crucial differences, although the nominal NiTi composition in the raw material is nearly the same, and gas atomization has been performed under constant conditions. Although it is favourable to use smallest available particles in order to achieve highest part resolution, the NiTi-M powder fraction with nominal diameters < 25 µm was used for the investigations presented here. This is due to the fact that sieving was a suitable method to separate the powder according to particle sizes for this material. Therefore, the portion used is well defined, as compared to NiTi-B powders.

3.2. Process results

Using the chosen powder portion NiTi-M with particles smaller than 25 µm in diameter, square shaped samples with a side length of 1.2 mm consisting of a single layer were generated from the powder bed. The powder bed thickness was set at 600 µm. In doing so, the squares did not come into contact with the substrate material. This was done for two reasons. On the one hand, the samples could be taken out of the powder bed easily without needing to loosen them from the substrate. This also assured that the shape memory properties of the samples were only influenced by the laser process itself and not by stresses or temperature influences for taking the samples off the substrate. Moreover, heat conduction into the powder bed is highly limited, compared to heat conduction into the fully dense substrate material [18]. Therefore, the heat induced by the laser process is used for layer generation from the powder to the highest possible amount. The resulting single layer thicknesses are the minimum thicknesses which can be gained within the powder volume when there is no support structure below it, as it is the case when part overhangs are created. The square samples were generated using varying laser power P_L and scanning velocity v_s. Micrographs of three samples of each parameter setting were taken, in which the thickness was measured five times per sample. The influence of the varied parameters on the layer thickness is shown in figure 2. In some cases, the parameter combination resulted in the generation of samples which could not be taken out of the powder bed without being damaged, respectively the sample only consisted of separated solidified melt droplets. For these samples, no thickness value can be determined, and therefore, there is an empty field in the matrix in figure 2. For the given values, the dotted line within the diagram bars respectively the transparent area above marks the standard deviation.

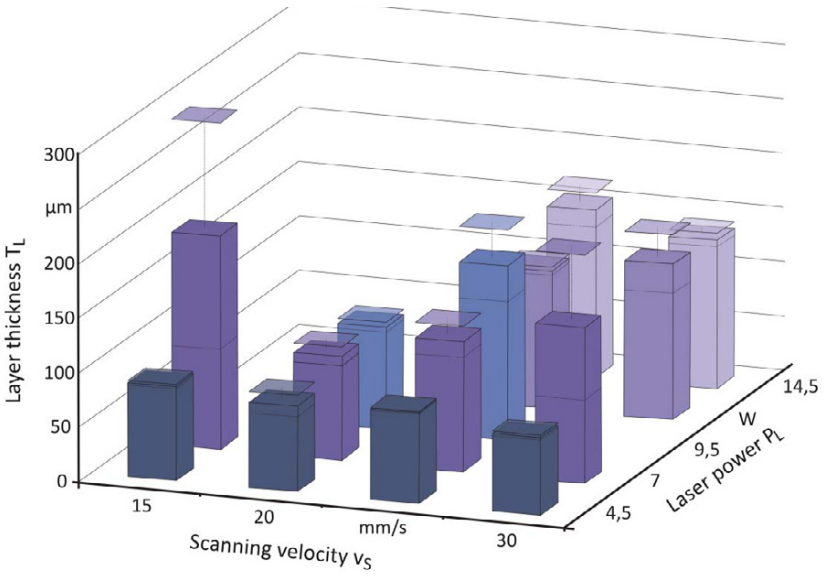

Fig. 2. Layer thickness plotted against varied process parameters

The thinnest layers could be generated by applying the lowest possible laser power P_L = 4,5. The thinnest layer areas of T_L = 55 µm can be found in the samples generated at a scanning speed of v_s = 30 mm/s. In all samples generated applying a laser power of P_L = 4,5, the standard deviation is comparably small, indicating that these samples show few defects, like material bulging or attached solidified droplets. Furthermore, layer thickness as well as standard deviation stay on a moderate level in all samples which could be generated at a scanning velocity of v_S = 20 mm/s. At laser powers P_L > 4,5 W, samples generated at comparably low scanning velocities show disrupted surface areas, due to the formation of droplet-like structures. When applying increased scanning speeds, layer thickness does not decrease as a result of decreased energy input in either case. In fact, where the set parameter combination leads to the formation of a less homogeneous sample surface, increased thicknesses and standard deviations were measured, indicating that the process is less stable here.

In order to evaluate the influence of process parameters on the transition temperature of the shape memory alloy, A_{peak} temperature was determined in DSC measurements. These were first performed on the untreated NiTi powder. One powder sample was repeatedly measured with every of the sample series. Therein, it was found that the difference in measured A_{peak} temperatures of the reference powder sample is above the range of the standard deviation measured in the samples of one sample serial. Due to the difference in the geometry of the samples (caused by surface defects, e. g.), it was not possible to use constant sample weights in between the sample series. Therefore, the standard deviation of DSC measurement results is not shown in figure 3, giving the A_{peak} temperatures of the laser sintered samples plotted against the varied process parameters. The value given for laser power P_L = 0 W and scanning velocity v_s = 0 mm/s is the transition temperature measured in the untreated powder, which is A_{peak} = 60.53 °C ± 2.17 °C.

In order to be able to show an A_{peak} modification as a result of the applied process parameters despite the comparably large system deviation, not only defect-free samples were measured. Moreover, the focus was on a reasonable change in laser energy input into the samples created at a constant laser power, which lead to scanning speeds as slow as v_s = 5 mm/s for lowest applicable laser power P_L = 4,5 W. When increasing the laser power, the scanning velocity was adapted respectively, in order to achieve a comparable energy input related to the given parameter combination at lower laser power.

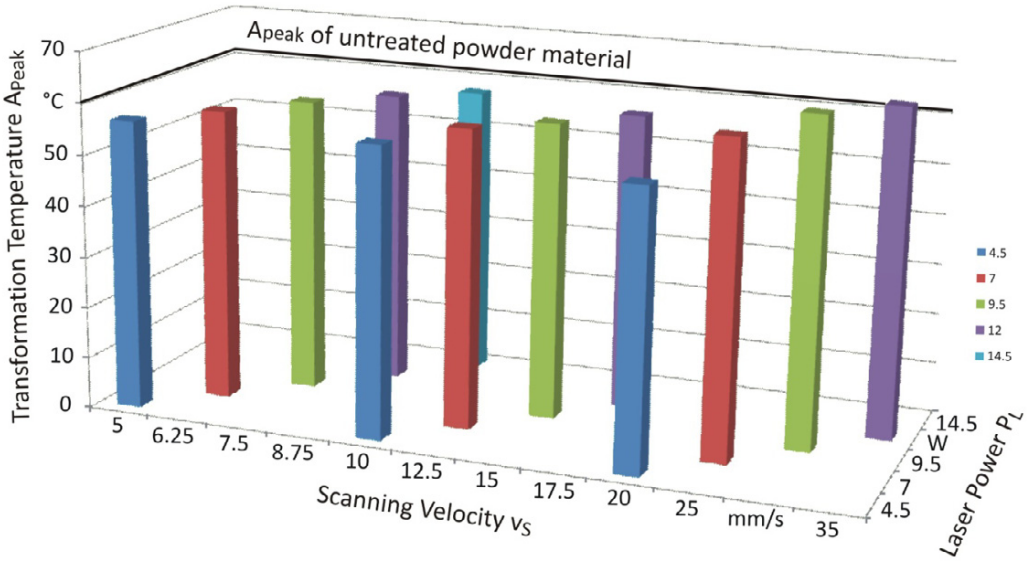

Fig. 3. A_{peak} temperatures of the untreated powder material and the laser sintered samples plotted against varied process parameters

Except from samples generated at $P_L = 4{,}5$ W, transition temperatures increase with increased scanning velocity if P_L is constant and therefore the overall laser energy is decreased. Comparing samples generated at similar energy input, A_{peak} increases with increased laser power and scanning velocity respectively. The absolute A_{peak} temperature decreased compared to the transition temperature of the powder for investigated samples within a parameter space spanned by $v_S \leq 20$ mm/s and $P_L \leq 12$ W. Outside these limits, transition temperatures are above A_{peak} of the powder material. This phenomenon can be explained by the co-existence of two competing processes. The first one is the selective vaporization of nickel from the NiTi matrix, which has been presumed by Meier et al. [13]. The loss of nickel leads to an increase in the transition temperature. The second one is oxygen pick up during the laser process, which leads to the formation of Titanium oxide. The relative amount of nickel within the NiTi matrix increases, leading to decreased transformation temperatures. This effect could also be observed by Hahn et al. [19]. As the interaction time of the elevated temperature NiTi material with the process atmosphere is higher at low scanning speeds, an increased oxygen pickup can occur. On the other hand, the necessary energy input to induce selective nickel vaporization is exceeded at increased laser powers, at least in center of the fibre laser beam of Gaussian energy deviation. Depending on which effect shows greater impact at a given parameter combination, transition temperature changes to the one or other direction. This indicates as well, that a parameter field can be found in which A_{peak} stays on the level of the powder material. However, this is only practical if a parameter combination can be found in which the sintering process is stable, with regard to the desired structure accuracy as well.

Besides the transition temperature, the size of the shape memory effect is of crucial interest. A crucial condition for the shape memory effect is the phase transformation ability. As the shape memory material consumes, respectively releases energy during phase transformation, this amount of energy can be used as a measure for transformation ability. In DSC measurement, the energy consumption of phase transition can be determined by

calculating the area integral spanned by the peak curve and the base line. The transition energy of the untreated powder material and the laser sintered samples is given in figure 4. The transition energy of the powder material, shown at $P_L = 0$ W and $v_S = 0$ mm/s, is $E_T = 27.44$ J/g ± 0.88 J/g.

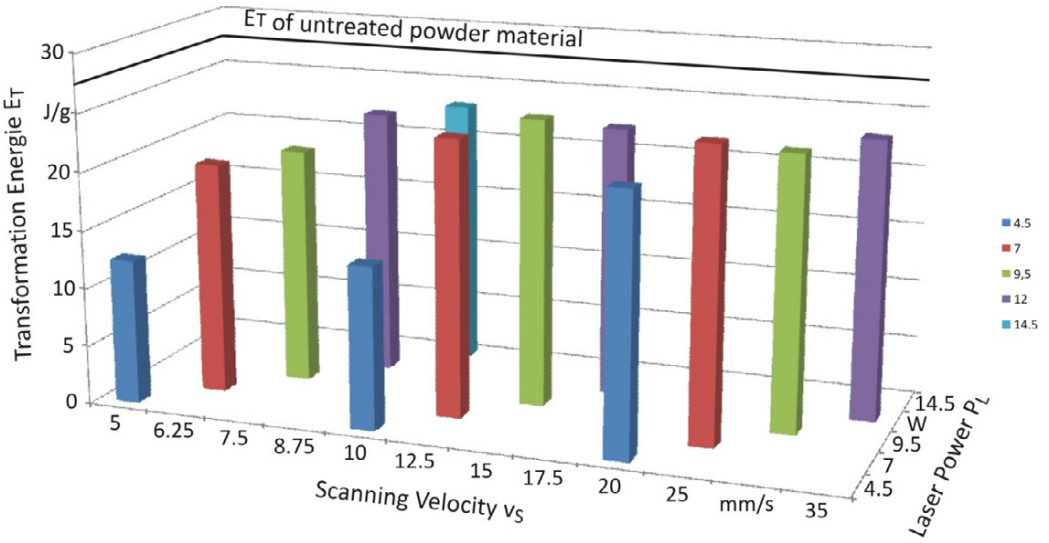

Fig. 4. Transformation energy E_T of the untreated powder material and the laser sintered samples plotted against varied process parameters

As a result of the applied laser power, the transition energy decreases in all samples. It is limited to 45.4 % to 91.5 % of the transition energy measured in the powder sample. There is a tendency that samples which show the strongest reduced transition temperatures show reduced transition energies as well. It is therefore assumed that in the laser process, the increase in oxygen content leads to the formation of a material phase volume which does not show the shape memory effect, respectively which is out of the range of the nickel to titanium ratio in which the shape memory effect can occur. The main part of the investigated samples, including those with increased transition temperatures, is within a range showing 83.7 % to 91.5 % of the initial transition energy. Therefore, it can be said that within a wide parameter range a reasonable amount of phase transformation ability of NiTi shape memory alloy can be preserved during the laser sintering process.

To show this transformation ability “at work”, wall-like structures consisting of a minimum width of 49.4 µm ± 6.1 µm and a height of 2 mm were generated from the powder bed. These structures were coiled up by wrapping them around a cotton bud, which is about 2 mm in diameter. When heating the coiled structures in water, they remember their stretched shape at about 55 °C. Figure 5 shows the structure as laser sintered on the substrate together with a blond hair for size comparison. Furthermore, it shows the coiled up structure and the stretched structure after warming. In the middle of the stretched structure, a kink is visible, which is in accordance with the edge of the wall structure, marking which way the structure was curled around the cotton bud.

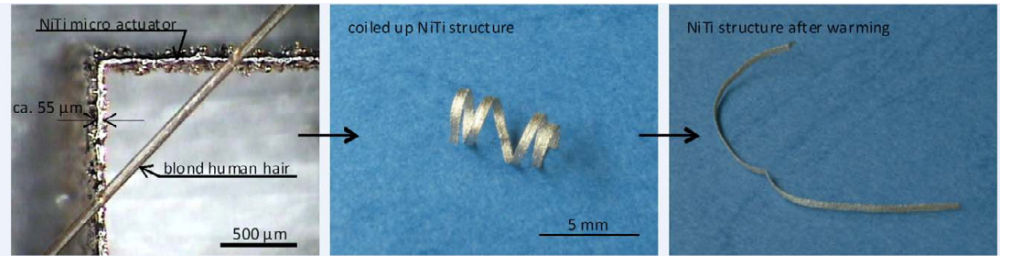

Fig. 5. Structure as sintered, curled up and stretched after heating in water

The curvature which can be seen in the stretched structure is a result of plastic deformation which occurred in curling the sample around the cotton bud against its kink direction, as this deformation surely extended the maximum of about 8 % so called pseudo plastic deformation, which can typically be found in NiTi shape memory alloys.

4. Conclusion and Outlook

It could not only be shown that fine NiTi powders can be processed using laser sintering to generate small structures in micrometer range. It was also demonstrated that in these structures the shape memory effect can be preserved within a reasonable field of process parameters. Moreover, a dependency of the shift of transition temperature from the process parameters in laser sintering could be shown for the first time, which is assumed to be a function of the addition of oxygen on the one hand and nickel vaporization on the other hand. Since these effects have a superposed impact, they can probably be used to control the transition temperature of shape memory structures built using laser sintering in a certain range around the transition temperature preset in the powder material. These results can contribute to the access of NiTi micro-actuators for technical and medical applications. Concerning the latter, it could already be shown that laser-generated NiTi micro- and nanostructures show good biocompatibility [19, 20].

Acknowledgements

The authors gratefully acknowledge partial funding of the presented work by the German Research Foundation (DFG) within the collaborative research center SFB Transregio 37, subproject C2.

References

1. P. Gümpel and S. Gläser. Formgedächtnislegierungen, Renningen, 2004, 1. 1
2. Y. Bellouard et al. SMST-1999, USA, 1999, 208.
3. D. E. Hodgson. SMST-2000, USA, 2000, 11.
4. K. Weinert and V. Petzoldt. Mat. Sci. Eng. (A) Vol. 378 (2004) 180.
5. A. von Busse et al. LANE-2004, Erlangen, 2004, 1113.
6. A. Schüssler and M. Strobel. SMST-2000, USA, 2000, 135.
7. C. Bonsignore. SMST-2000, USA, 2000, 519.
8. M. Mertmann. Formgedächtnislegierungen, Renningen, 2004, 55.
9. N.N. www.memry.com; 24.04.2010

10. N.N. www.saes-getters.com; 24.04.2010
11. N. Seitz. Formgedächtnislegierungen, Renningen, 2004, 130.
12. K. Freislinger Luehrs. SMST-2003, USA, 2003, 435.
13. H. Meier et al. Advanced Research in Virtual and Rapid Prototyping, 2009, p.233.
14. S. Dudziak et al. International Congress on Applications of Lasers & Electro-Optics – ICALEO 07, USA, M606.
15. K. J. Khalil-Alafi et al. Acta Materialia 50(17) (2002) 4255.
16. J. Frenzel et al. Journal of Alloys and Compounds 385 (2004) 214.
17. J. Mentz et al. Mat. Sci. Eng. (A) Vol. 491 (2008) 270.
18. V. Schütz et al. Proceedings of the LIM, 2009, 483.
19. A. Hahn et al. J. Nanoparticles Res. (published online 12.03.2010, DOI 10.1007/s11051-009-9834-4).
20. S. Dudziak et al. Euromat 2009, poster, Symp. B53, 2009.